TU Delft

Delft University of Technology

Document Version
Final published version

Licence
CC BY

Citation (APA)
Kruisdijk, E., Corbera-Rubio, F., Müller, S., Schoonenberg, F., Laureni, M., Nijboer, M., & van Halem, D. (2026). pH-based control of NH_4^+ and Mn^{2+} oxidation sequence in low-oxygen groundwater filters. *Water Research*, *293*, Article 125436. https://doi.org/10.1016/j.watres.2026.125436

Important note
To cite this publication, please use the final published version (if applicable).
Please check the document version above.

Copyright
In case the licence states “Dutch Copyright Act (Article 25fa)”, this publication was made available Green Open Access via the TU Delft Institutional Repository pursuant to Dutch Copyright Act (Article 25fa, the Taverne amendment). This provision does not affect copyright ownership.
Unless copyright is transferred by contract or statute, it remains with the copyright holder.

Sharing and reuse
Other than for strictly personal use, it is not permitted to download, forward or distribute the text or part of it, without the consent of the author(s) and/or copyright holder(s), unless the work is under an open content license such as Creative Commons.

Takedown policy
Please contact us and provide details if you believe this document breaches copyrights.
We will remove access to the work immediately and investigate your claim.

This work is downloaded from Delft University of Technology.

Water Research 293 (2026) 125436

Contents lists available at ScienceDirect

Water Research

journal homepage: www.elsevier.com/locate/watres

pH-based control of NH_4^+ and Mn^{2+} oxidation sequence in low-oxygen groundwater filters

Emiel Kruisdijk [a,b,1,*], Francesc Corbera-Rubio [a,1], Simon Müller [a], Frank Schoonenberg [c], Michele Laureni [a], Melanie Nijboer [c], Doris van Halem [a]

[a] Delft University of Technology, Faculty of Civil Engineering and Geosciences, Department of Water Management, Stevinweg 1, 2628 CN Delft, the Netherlands
[b] Eawag, Swiss Federal Institute of Aquatic Science and Technology, Ueberlandstrasse 133, CH-8600 Dübendorf, Switzerland
[c] Vitens N.V., Oude Veerweg 1, 8019 BE Zwolle, the Netherlands

HIGHLIGHTS

- Three separate filters were designed to sequentially remove Fe^{2+}, Mn^{2+}, and NH_4^+.
- Sequential oxidation was controlled by adapting O_2 and pH in influent groundwater.
- The sequence of NH_4^+ before Mn^{2+} oxidation could be reversed based on pH.
- MnOx was reduced via NO_2^- when O_2 was limited and MnOx was present.
- Interactions between NH_4^+ and Mn^{2+} influenced their oxidation rates.

GRAPHICAL ABSTRACT

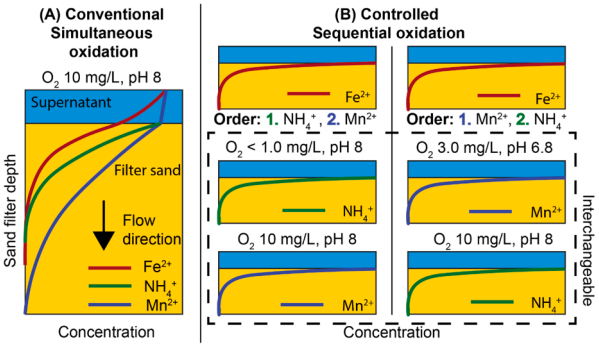

ARTICLE INFO

Keywords:
Drinking water
Groundwater
Sand filtration
PHREEQC, PEST

ABSTRACT

Iron (Fe^{2+}), manganese (Mn^{2+}), and ammonium (NH_4^+) are the three most common contaminants in anaerobic groundwater and are typically removed in rapid sand filters in a series of simultaneous, uncontrolled, and interconnected redox reactions. In this study, we demonstrated separation of these oxidation processes, including reversing the order of NH_4^+ and Mn^{2+} oxidation, allowing Mn^{2+} to oxidize before NH_4^+. To achieve this uncommon sequence, the filter was operated with low O_2 concentrations (~0.02 mmol/L, ~0.5 mg/L) and a high pH (~8). Under these conditions, Mn^{2+} oxidation is consuming all available O_2, suppressing the occurrence of NH_4^+ oxidation. In the filter with low O_2 (0.08 mmol/L, ~3 mg/L) and low pH (~6.8), the opposite was observed, as Mn^{2+} oxidation was delayed under these conditions, resulting in complete O_2 consumption by NH_4^+-oxidizing bacteria. Reactive transport modelling and parameter estimation revealed that Mn^{2+} oxidation is one order of magnitude faster in absence of NH_4^+ oxidation (1.4×10^{-2} vs 2.5×10^{-3} mmol/L), whereas NH_4^+ oxidation seemed to be accelerated by simultaneous Mn^{2+} oxidation (6.8×10^{-3} vs 2.9×10^{-2} s^{-1}). This interconnection between Mn^{2+} and NH_4^+ oxidation was further emphasized by the observation of Mn^{2+} release in the presence of NO_2^-. In conclusion, this study has shown that a shift from conventional aerated groundwater treatment to

* Corresponding author.
E-mail address: e.kruisdijk@tudelft.nl (E. Kruisdijk).
[1] Shared co-authorship.

https://doi.org/10.1016/j.watres.2026.125436
Received 18 September 2025; Received in revised form 24 December 2025; Accepted 20 January 2026
Available online 20 January 2026
0043-1354/© 2026 The Author(s). Published by Elsevier Ltd. This is an open access article under the CC BY license (http://creativecommons.org/licenses/by/4.0/).

sequential oxidation in separate filters offers (i) a more controllable system, (ii) the potential to optimize the rates of each oxidation process separately, which would ultimately result in higher flows and less backwashing.

1. Introduction

About half the people worldwide rely on groundwater as their primary source for drinking water (UNESCO, 2022). The largest part of the abstracted groundwater for drinking water purposes is anoxic, as biological and chemical processes in aquifers often consume all the available oxygen (O_2) (Fetter et al., 1999). Under these anoxic conditions, iron(II) (Fe^{2+}) and manganese(II) (Mn^{2+}) generally enter the groundwater due to reduction of Fe and Mn minerals present in the aquifer (Gounot, 1994; Kappler et al., 2021), while ammonium (NH_4^+) is often formed as a product of organic matter degradation (Appelo and Postma, 2004). These solutes in anaerobic groundwater must be removed prior to human consumption, as they cause, adverse health effects, microbial re-growth and clogging in the distribution system, as well as altered color, taste, and odor (Tekerlekopoulou et al., 2013).

Rapid sand filters (RSF) are widely used for groundwater treatment around the world (Corbera-Rubio, Goedhart, et al., 2024). After abstraction, groundwater is first oxidized by means of aeration or the addition of chemical oxidants, after which the water is directed to the RSF. RSF effectively removes Fe^{2+}, Mn^{2+}, and NH_4^+ from the water through a series of simultaneous, uncontrolled oxidation reactions. Fe^{2+} can be oxidized via chemical homogeneous (Stumm and Lee, 1961) or heterogeneous (Tamura, 1976) oxidation, as well as biological heterogeneous oxidation (Emerson and De Vet, 2015). Only chemical heterogeneous (Davies and Morgan, 1989) and biological heterogeneous oxidation (Bruins et al., 2015) are relevant for Mn^{2+}, as homogeneous Mn^{2+}oxidation rates are negligible during the relatively short residence time in RSF (Diem and Stumm, 1984). The quick hydrolysis of the formed oxidized forms of Fe^{2+} and Mn^{2+}- $Fe^{3+}$and Mn^{3+}/Mn^{4+}, respectively - results in the precipitation of Fe- and Mn-hydroxides. The formed Fe- and Mn-hydroxides form a coating on the grains during heterogeneous oxidation of Fe^{2+} and Mn^{2+}, as a result colloidal Fe(III) and Mn(IV) is negligible compared to treatments in which homogeneous oxidation is induced by adding oxidants.

Complete NH_4^+ oxidation, known as nitrification, is a solely biological process in RSFs which results in the conversion of NH_4^+ to nitrate (NO_3^-) via the intermediary nitrite (NO_2^-) (Tatari et al., 2013).

During RSF operation, Fe^{2+}, Mn^{2+}, and NH_4^+ oxidation generally occurs simultaneously, although Fe^{2+}oxidation is energetically most favourable, followed by NH_4^+ and Mn^{2+}oxidation. In some specific cases, sequential Fe^{2+} and NH_4^+ (Corbera-Rubio, Kruisdijk, et al., 2024; Müller et al., 2024) or Fe^{2+} and Mn^{2+} oxidation (Kruisdijk, van Breukelen, et al., 2024) is observed. In our previous work, we showed that sequential Fe^{2+} and Mn^{2+}oxidation resulted in homogeneous Fe-oxide coated sand grains in the top section of the filter, and Mn-oxide coated sand grain at the bottom (Kruisdijk, van Breukelen, et al., 2024). This contrasts with the usual mixed Fe-Mn coated sand grains found in filters with simultaneous Fe^{2+} and Mn^{2+}oxidation. Grains with a homogeneous Fe or Mn-oxide coating result in accelerated heterogeneous oxidation rates as oxidation is not limited by the available oxide surface and have a higher potential value for reuse.

We hypothesize that sequential Fe^{2+}, NH_4^+, and Mn^{2+}oxidation in separate filters can be a major advantage to control and optimize oxidation processes, as the separate filters provides greater potential for operational optimization through adjustments in flow rates, pH of influent water, aeration, and other process parameters. Furthermore, complex intertwined processes that may lead to system failure are avoided, such as the inhibition of NH_4^+ oxidation by Fe^{3+}-flocs formed during Fe^{2+} oxidation (Corbera-Rubio et al., 2024). Therefore, this allows for the determination of conditions that promote the most efficient RSF operation, ensuring maximum flow rates and prolonged runtimes.

Müller et al. (2024) studied two filter setups and achieved sequential oxidation of Fe^{2+} and NH_4^+ in the filter setup that was only partially aerated (resulting in a lower pH and O_2 concentration) compared to simultaneous oxidation in the filter setup that was intensively aerated. We hypothesize that the limited O_2 concentrations allowed only the most energetically favourable oxidation process to occur, after which O_2 was depleted and NH_4^+ oxidation could not occur. In the current study, we introduce a novel approach for anaerobic groundwater treatment, where Fe^{2+}, Mn^{2+}, and NH_4^+ are oxidized sequentially over three separate filters. O_2 availability was kept limited in each filter and the optimal pH was set for the highest oxidation rate for each specific process. We provide a framework for potentially more controllable and efficient groundwater treatment compared to traditional single-filter treatment, although full-scale operational performance, energy use, and financial feasibility remain to be evaluated.

This was investigated with three separate filter sequences operated at pilot-scale with natural groundwater. In all studied oxidation sequences, Fe^{2+} is removed first, and the order of NH_4^+ and $Mn^{2+}$was studied (i) simultaneous oxidation in a fully aerated filter, (ii) sequential oxidation of Mn^{2+} in the pre-filter and NH_4^+ in the post filter, and (iii) sequential oxidation of NH_4^+ in the pre-filter and Mn^{2+} in the post filter. These sequences were obtained by adjusting the pH and O_2 concentrations in the pre-filter. A combination of reactor transport modelling and parameter estimation was used to determine oxidation rates, as well as identify coupled processes.

2. Methods

2.1. Experimental setup

Fig. 1 shows the experimental setup consisting of a full-scale rapid sand filter (RSF) and five pilot-scale filters. Note that the influent water to all filters was aerated, and no oxidants were dosed to initiate oxidation. The experiments were conducted at a Dutch drinking water treatment plant with abstracted groundwater abstracted from an anaerobic aquifer. The raw water had a mean pH of 6.72±0.06, and contains CH_4, Fe^{2+}, NH_4^+ and Mn^{2+} with average concentrations of 14.1 ± 2.8, 26.7 ± 1.5, 2.19±0.05 and 0.32±0.02 mg/L, respectively (see SI.1).

Three filter sequences were studied: (i) simultaneous NH_4^+ and Mn^{2+} oxidation in filter F1, (ii) sequential oxidation of Mn^{2+} in pre-filter F2 and NH_4^+ oxidation in post-filter F3, and (iii) sequential oxidation of NH_4^+ in pre-filter F4 and post filter F5. The full-scale experimental RSF was the first filter for all three filter sequences, and operated as described by Müller et al. (2024). Before entering the filter, CH_4 was removed by membrane degassing under anoxic conditions. This process both generates energy from the recovered CH_4 and reduces the carbon footprint, as CH_4 is normally released into the atmosphere. The water was subsequently mildly aerated by means of a one-step cascade aeration on top of the ±20 cm-high supernatant water layer on the full-scale RSF. The filter bed height was 2.35 m and consisted of coarse quartz sand (1,7–2,5 mm). The average filtration rate was 10 m/h. Membrane degassing and mild aeration led to a filter that was operated under relatively low pH (~6.9) and dissolved O_2 concentrations (~5 mg/L). Operation under these conditions resulted in mostly biological Fe^{2+}oxidation, less Fe-floc and more Fe coating formation, and negligible $NH_4^+$and Mn^{2+} oxidation (Müller et al., 2024). The effluent water from this filter was distributed to the pilot-scale filters. Table 1 shows the water composition of the influent after aeration and membrane degassing and effluent water of the Fe-removing RSF. Fe^{2+} was almost completely oxidized and removed, while the oxygen concentration dropped to 1.15 mg O_2/L.

In filter F1, the effluent water from the full-scale rapid sand filter was fully aerated in a column with pall rings of 1 inch with a bed height of 1.4 m with counter-current airflow. This resulted in an increased pH (~8), and O_2 concentration (~10 mg/L) to facilitate complete nitrification and Mn^{2+}oxidation in one filtration step. To accomplish the Mn^{2+}-NH_4^+ oxidation sequence, O_2 concentrations were kept as low as possible in pre-filter F2, and a base was dosed (NaOH) to increase the pH (<1.0 mg/L O_2, pH 8) to promote Mn^{2+} oxidation and inhibit NH_4^+ oxidation. The effluent water was fully aerated in a pall ring column with counter-current airflow before entering post-filter F3 to remove NH_4^+. For the NH_4^+-Mn^{2+} oxidation sequence, effluent water from the full-scale RSF was directly injected into the supernatant of pre-filter F4, resulting in a low pH and O_2 concentrations (pH 6.8, 3.0 mg/L, respectively). The effluent water was fully aerated before entering post filter F5, aimed to remove Mn^{2+}.

All filter columns had an inside diameter of 15 cm. The filter beds consisted of anthracite (grain size between 1.4–2.5 mm), of which approximately 10 L of anthracite was re-used from a Mn^{2+}oxidizing filter and 30 L was virgin anthracite resulting in a bed height of about 190 cm. The two types of anthracite were homogenously mixed before filling the column. The re-used anthracite grains contained a substantial Mn-oxide coating. All filters were operated with a flow of approximately 75 L/h, which corresponds to a filtration rate of 8.4 m/h assuming a porosity of 0.45. Filters F1, F4 and F5 were operated for 28 days, and filter sequence F2 and F3 was operated for 93 days. The filters were not backwashed, except for filter F2, which was backwashed on days 61, 75, and 82 to prevent clogging.

2.2. Water sampling and analysis

Water samples were taken from the full-scale RSF and the pilot-scale filters via sample points over the depth of the filter. Samples for Fe^{2+} and Mn^{2+} were filtered over a 0.45 μm disc filter and collected in a 330 mL bottle filled with 100 mL sample and 1.0 mL of HNO_3 to ensure a pH ≤ 2 for sample preservation. Particulate Fe and Mn were not measured because (i) Fe^{2+} oxidation in Ca- and Si- containing groundwaters is assumed to produce only filterable particles (Kaegi et al., 2010; Voegelin et al., 2010), and (ii) previous studies found particulate Mn in RSF to be negligible (Haukelidsaeter et al., 2023, 2024). Samples for NH_4^+, NO_2^-, NO_3^-, dissolved O_2, and pH were collected without filtration in a 550 mL bottle with a cone inside the cap. The cone pushes excess liquid out while closing, preventing air from being trapped inside the sample bottle. All sample bottles were cooled between 2–8 °C and transported to the laboratory. Fe^{2+} and Mn^{2+} were analysed using inductively coupled plasma mass spectrometry (Thermo Scientific iCAP RQ). NH_4^+, NO_2^-, and NO_3^-were analysed with a discrete analyser (Thermo Scientific AquaKem 600). Dissolved O_2 and pH were measured with sensors in the lab (WTW inoLab Multi 9630 IDS). In addition, to check and adjust process conditions, dissolved oxygen and pH were measured on-site using sensors (WTW Multi 3630 IDS field set).

Table 1
Overview of the influent after aeration and membrane degassing and effluent water composition of the full-scale Fe^{2+}oxidizing rapid sand filter on the day of the measured height profile, where the major water quality changes are highlighted with a grey background.

	Influent RSF	Effluent RSF
pH (-)	6.9	6.7
O_2 (mg/L)	4.6	1.2
NO_3–N (mg/L)	<0.3	<0.3
NH_4–N (mg/L)	2.3	2.0
Fe (mg/L)	28	<0.1
Mn (mg/L)	0.3	0.3
Alkalinity (mg/L)	280	unknown
PO_4 (mg/L)	0.28	<0.1
SO_4 (mg/L)	4.5	4.56
Ca (mg/L)	74	74
Mg (mg/L)	4.2	4.1
Si (mg/L)	8.8	8.7
CH_4 (μg/L)	300	unknown

2.3. Modelling approach

PHREEQC (Parkhurst and Appelo, 2013) was used to simulate coupled processes in the filters and PEST (Doherty, 1994) was used to derive unknown parameters in the used oxidation rate equations. This is a similar modelling approached as performed by Kruisdijk, van Breukelen, et al. (2024). We simulated the filter bed as a 1-dimensional pathway. This pathway consisted of 195 cells of 1 cm length. The flow velocity in the filter bed was calculated by dividing the flow of 75 L/h by the surface area of the column multiplied with the assumed porosity of 0.3. The timestep per cell was calculated by dividing the cell length by the flow velocity. The measured influent water composition after aeration was used as the initial solution for each pilot-scale filter. We did not simulate hydrodynamic dispersion to reduce complexity and shorten run-times. An overview of the kinetic processes simulated can be found in Table 2. PEST was used to estimate the unknown parameters in these

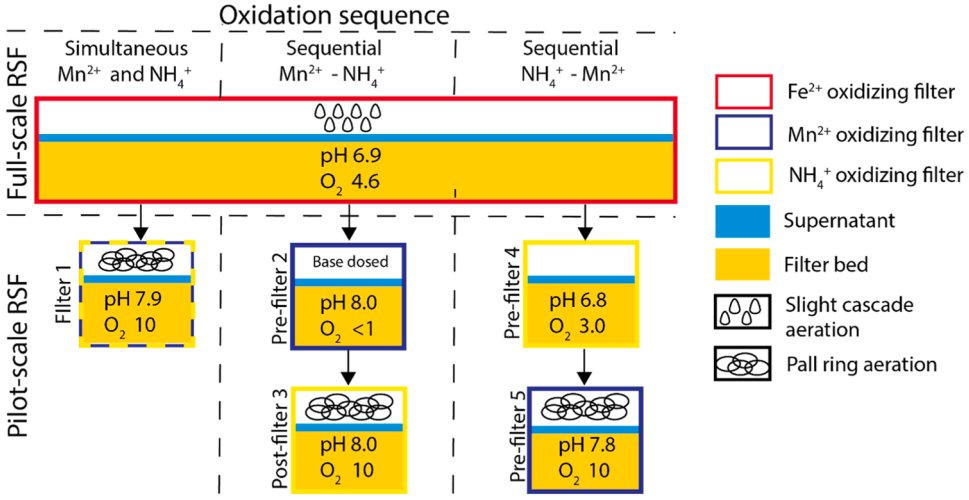

Fig. 1. Overview of experimental setup, with on top the full-scale rapid sand filter, and on the bottom the three different treatments. The outline of each box shows which oxidant is removed in each filter, the inside of the box shows the pH and O_2 concentration in mg/L during operation. The symbols on top of the filter bed represent the type of aeration.

Table 2
Kinetic processes simulated in the model, their chemical formulas, and corresponding rate equations. Source equation 1: Davies and Morgan (1989).

Eq.	Kinetic process	Chemical formula	Rate equation
1	Heterogeneous Mn^{2+} oxidation	$Mn^{2+}_{ads} + \frac{1}{2}O_2 + H_2O \leftrightarrow MnO_2 + 2H^+$	$r_{Mn-hetero} = -k[Mn^{2+}ads]P_{O_2}$
2	Complete nitrification	$NH_4^+ + 2O_2 \leftrightarrow NO_3^- + 2H^+ + H_2O$	$r_{nitrification} = -k_{nitr}[NH_4^+]$
3	NH_4^+ oxidation	$NH_4^+ + 1.5\ O_2 \leftrightarrow NO_2^- + H_2O + 2H^+$	$r_{NH_4} = -k_{NH4}[NH_4^+]$
4	NO_2^- oxidation	$NO_2^- + 0.5\ O_2 \leftrightarrow NO_3^-$	$r_{NO_2} = -K_{NO_2}[NO_2^-]$
5	NO_2^- -induced Mn-oxide reduction	$NO_2^- + MnO_2 + 2H^+ \leftrightarrow Mn^{2+} + NO_3^- + H_2O$	$r_{Mn-red} = -K_{Mn-red}[NO_2^-]$

kinetic oxidation processes (Mn^{2+}ads, k_{nitr}, k_{NH4}, and k_{NO2}) by optimizing the fit between the simulated and observed concentrations using the Gauss-Marquardt-Levenberg method. This method was executed simultaneously for the oxidation of Fe^{2+}, Mn^{2+}, and NH_4^+ in a single PEST run for each RSF model.

Fe^{2+} oxidation was simulated similarly as in Kruisdijk, van Breukelen, et al. (2024) where this filter is represented as RSF-S3, while new simulations were performed to assess the water quality changes in the Mn^{2+} and NH_4^+ oxidizing filters. For these filters, only reactions in the filter bed were simulated because no major reactions were observed and expected to happen in the supernatant. Furthermore, nitrification was simulated as two-steps - NH_4^+ oxidation and NO_2^- oxidation, - in the columns where we hypothesized that complete nitrification was not occurring. More information about the modelling approach in Kruisdijk, van Breukelen, et al. (2024).

The PHREEQC models plus the corresponding database, datafiles, and python scripts for visualization are available on GitHub: https://github.com/emielkruisdijk/Sequential_oxidation_2025/.

3. Results

3.1. Fe^{2+} oxidation in the full-scale RSF

Fig. 2 shows the simulated and observed concentrations in the full-scale Fe^{2+}-oxidizing rapid sand filter (RSF). Fe^{2+} oxidation was stimulated to occur in the filter bed instead of conventionally in the supernatant water. This was achieved by limiting aeration to maintain low O_2 concentrations (4.6 instead of ±10 mg/L) and a relatively low pH (6.9 instead of ±8) and keeping the supernatant water level low (20 cm instead of the usual 40 cm). This reduced the rate of homogeneous Fe^{2+} oxidation rate in the supernatant water almost 700 times (Stumm and Lee, 1961). These measures resulted in a Fe^{2+} concentration of approximately 0.4 mmol/L at the entrance of the filter bed. After complete Fe^{2+} oxidation in the filter bed, O_2 was close to depletion (±1 mg/L). The low oxygen concentration, combined with the relatively high filtration rate of 10 m/h, prevented NH_4^+ and Mn^{2+} oxidation to occur.

3.2. Simultaneous NH_4^+ and Mn^{2+} oxidation

Fig. 3 shows that NH_4^+ and Mn^{2+} oxidation occurred simultaneously in the fully aerated filter F1, resulting in decreasing NH_4^+, Mn^{2+}, and O_2 concentrations, increasing NO_3^- concentration, and a lower pH. The influent water reached close to O_2 saturation (±10 mg/L) in a counter-current air flow pall ring column before entering the pilot-scale filter, which additionally resulted in a pH increase to 8.0 due to CO_2 stripping. All processes occurred in the first 50–70 cm of the filter bed, after which concentrations stabilized.

The rate equations with the estimated parameters (Mn^{2+}ads, k_{nitr}) enable accurate simulation of NH_4^+ and Mn^{2+} oxidation. The simulated O_2 and NO_3^- concentrations, as well as pH, are coupled to the oxidation of NH_4^+ and Mn^{2+}. Their simulated trends fit the observed measurements well, while the concentrations are slightly off. These slight deviations are likely due to higher NH_4^+ concentrations in the influent water than monitored, which would explain the overestimation of NO_3^- concentration as well as the underestimation of O_2 concentration and pH. Instrument inaccuracy for O_2 and pH measurements may have contributed to this result as well.

Fig. 4 shows the percentage of NH_4^+ and Mn^{2+} concentrations removed in the pall rings prior to filter F1 during the experiment. While initially (first ~20 days), NH_4^+ removal was only observed in the filter bed, in weeks, removal also started to happen in the pall rings. With a steady increase, 90 % oxidation was observed after 133 days, meaning that NH_4^+ removal was almost complete prior to the water reaching the filter bed. A similar, but delayed, trend was observed for Mn^{2+} removal, with approximately 50 % removal by the pall rings after133 days. On day 68, the system was switched off for at least one full day, which seems to have resulted in temporary drop in NH_4^+ and Mn^{2+} removal (red dotted line in Fig. 4). The onset of NH_4^+ and Mn^{2+} oxidation in the pall rings suggests that surface limitation is not an issue in sand filters, as the surface area of pall rings is orders of magnitude smaller than that of sand.

3.3. Sequential Mn^{2+} and NH_4^+ oxidation

In pre-filter F2, the influent water was mildly aerated (4.6 mg O_2/L = 0.14 mmol O_2/L). Consequently, CO_2 was only partly stripped, which resulted in a relatively low pH. The influent water pH was raised to 7.8 by dosing sodium hydroxide. Fig. 5A shows that these conditions resulted in Mn^{2+} oxidation, while NH_4^+ oxidation was negligible. However, after full aeration in subsequent post filter F3 (Fig. 5B), complete nitrification occurred. The simulations accurately follow the observed trends and concentrations, except for the O_2 concentrations where simulated concentrations were slightly higher than observed likely for the same reasons as mentioned for the fully aerated filter F1.

Precipitation of minerals (=scaling) was observed in pre-filter F2 and

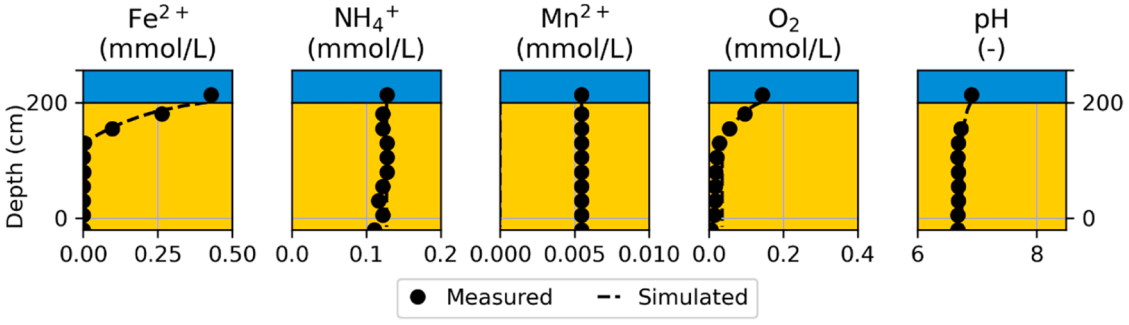

Fig. 2. Observed and simulated solute concentrations and pH with depth in the supernatant and filter bed for the full-scale rapid sand filter (adapted from Kruisdijk 2024).

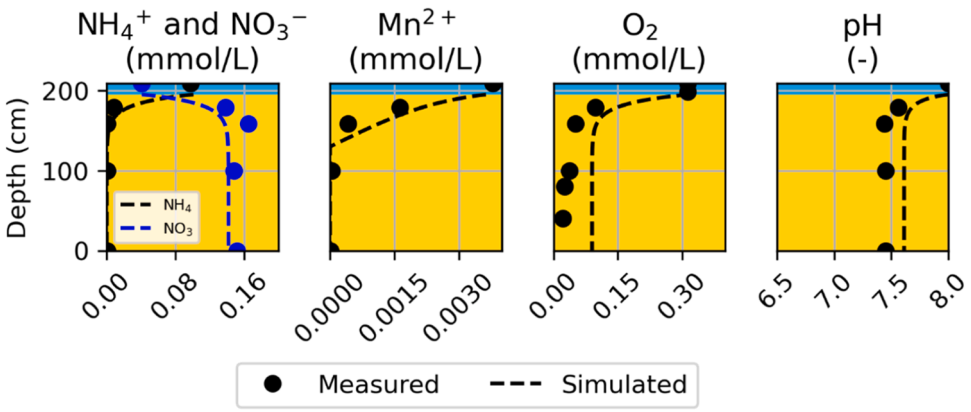

Fig. 3. Observed and simulated concentrations and pH in fully aerated filter F1, in which simultaneous NH_4^+ and Mn^{2+} oxidation was stimulated.

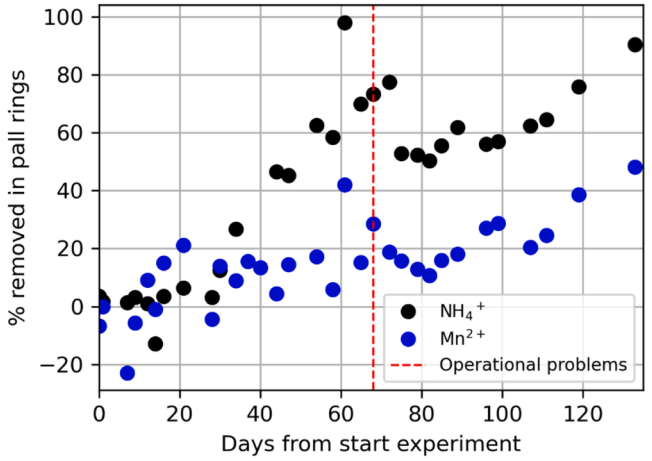

Fig. 4. Percentage of NH_4^+ and Mn^{2+} concentrations removed during pall ring aeration prior to filter F1 over the duration of the experiment.

caused operational problems resulting in more clogging and thus, backwashing. The most severe scaling occurred especially close to the sodium hydroxide dosing tube, where we expected locally high pH due to incomplete mixing. SI.2 shows the simulated saturation index (SI) of two common carbonate precipitates, calcite ($CaCO_3$) and rhodochrosite ($MnCO_3$), based on the average influent groundwater composition (SI. 1) at increasing pH values. Both SIs reach equilibrium (SI=0) between pH 7.2–7.3 and become supersaturated at higher pH highlighting potential mineral precipitation. The SI of calcite increases most substantially. Rhodochrosite precipitation would have caused a decrease in Mn^{2+} concentrations, which is unlikely to have happened, since Mn^{2+} concentrations in the supernatant water were very similar to the other pilot filters that did not cope with clogging issues.

3.4. Sequential NH_4^+ and Mn^{2+} oxidation

In pre-filter F4, influent water was only slightly aerated resulting in O_2 concentrations of around 3.9 mg/L and a relatively low pH of 6.8. These conditions promoted NH_4^+ oxidation, but only partially as O_2 concentrations were not sufficient to oxidize all NH_4^+ (Fig. 6A). Mn^{2+} oxidation was not observed; instead Mn^{2+} concentrations increased. The pH remained somewhat stable. The effluent water was fully aerated before entering the post filter F5, using pall rings and counter current air flow resulting in 11 mg/L O_2 (=0.35 mmol/L) and a higher pH (=7.9). In this filter, both NH_4^+ and Mn^{2+} were fully removed, resulting in a decrease in O_2 concentration and a lower pH (Fig. 6B).

The two sequential filters show a good fit between the observed and simulated concentrations. Only the pH dropped substantially in the second filter (Fig. 6B), a change that was not captured by the simulation - similar to aerated filter F1.

Simulating complete nitrification in a single-step (equation 2) did not result in a good fit for the simulated and observed NH_4^+ and NO_3^- concentrations, and most importantly, the increasing Mn^{2+} concentrations were not simulated (SI.3). The only reasonable way to simulate increasing Mn^{2+} concentrations was to couple it to NO_2^- oxidation. Vandenabeele et al. (1995) observed this process in laboratory batch experiments with similar conditions to RSF. We added this process (equation 5) and two-step nitrification (equations 3 and 4) and simulated these processes using the model (Fig. 7A). Simulated and observed concentrations showed a good fit. To achieve an accurate model fit with the observed Mn^{2+} concentrations, NO_2^- concentrations are maximally 0.032 mmol/L after O_2 is fully depleted. NO_2^- was observed in the samples, but not in the same concentration range as simulated. Note that in the obtained water samples probably all NO_2^- was converted to NO_3^- due to the high reactivity of the NO_2^- and the low concentrations of O_2 available in the samples. Therefore, we assume that the sum of the simulated NO_2^- and NO_3^- concentrations represent the observed NO_3^- concentrations in the samples.

To investigate the influence of O_2 limitation on Mn-oxide reduction, the filter operation of pre-filter F4 was temporarily adjusted to full aeration, resulting in a higher pH (=7.33) and O_2 concentrations (9.2 mg/L). Fig. 7B shows the results of this adaptation to the observed concentrations over the filter bed. NH_4^+ is fully depleted within the first 80 cm and converted to NO_3^-. Mn^{2+} oxidation is occurring resulting in complete removal, instead of the Mn^{2+} mobilization observed in O_2 limited conditions. This strongly indicates that the Mn-oxide reduction observed in F4 is a result of O_2 limitation and likely coupled to NO_2^- presence.

3.5. Parameter estimation

Table 3 shows the estimated first order rate constants for NH_4^+ oxidation and adsorbed Mn^{2+} (which is a proxy for the heterogeneous Mn^{2+} oxidation rate), their 95 % confidence intervals, and the influent pH and O_2 concentrations. The estimated parameters reflect the behaviour of the filter columns under the specific conditions but should not be interpreted as having predictive skill outside this dataset.

First order complete nitrification rate constants ranged between 6.8 $\times$ 10^{-3} - 3.2 $\times$ 10^{-2} s^{-1}, while adsorbed Mn^{2+} ranged between 1.2 $\times$ 10^{-3} −1.4 $\times$ 10^{-2} mmol/L. In fully aerated filter F1, NH_4^+ and Mn^{2+} oxidation occurred simultaneously with an estimated first-order NH_4^+ oxidation rate constant of 3.5 $\times$ 10^{-2} s^{-1} and adsorbed Mn^{2+} of 1.2 $\times$ 10^{-3} mmol/L. In pre-filter F2, with partial aeration and high pH, Mn^{2+} oxidation was about one order of magnitude faster (1.4 $\times$ 10^{-2} mmol/L), despite the slightly lower pH (7.74). In pre-filter F4, with low

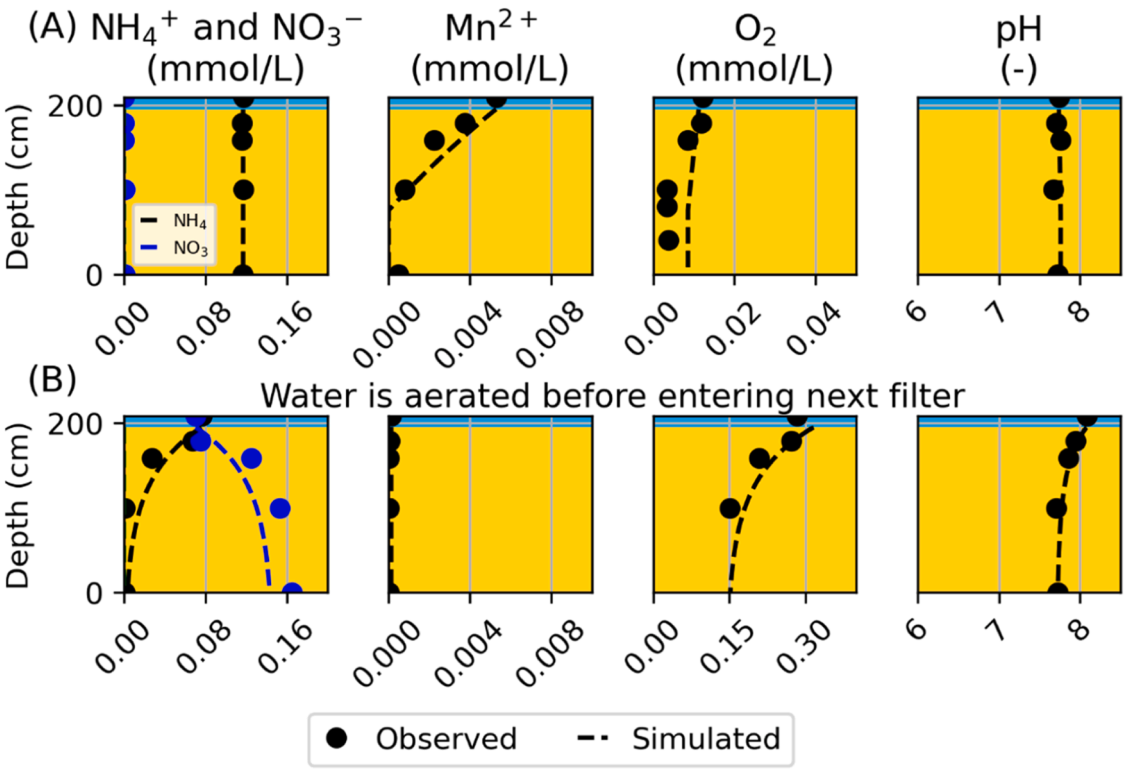

Fig. 5. Observed and simulated concentrations and pH for sequential Mn^{2+} and NH_4^+ oxidation in (A) pre-filter F2, and (B) post filter F3.

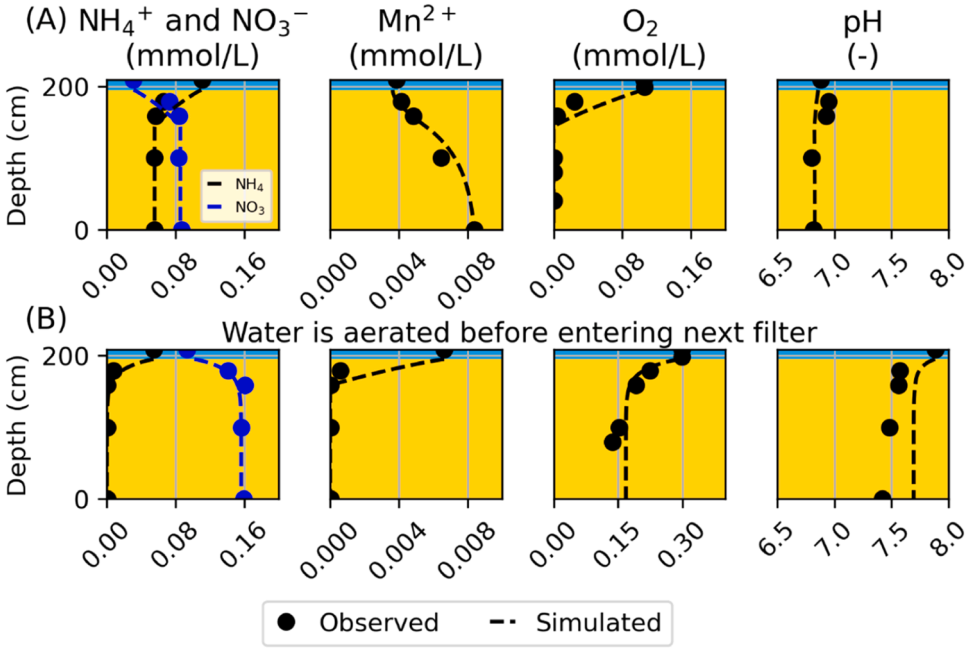

Fig. 6. Observed and simulated concentrations and pH for sequential NH_4^+ and Mn^{2+} oxidation in (A) pre-filter 4, and (B) post filter F5.

pH and partial aeration, NH_4^+ oxidation was about one order of magnitude slower, compared to the aerated filter F1 (5.5×10^{-3} s^{-1}).

Post-filters F3 and F5 (Table 3) had similar process conditions as the fully aerated filter F1. Nonetheless, NH_4^+ oxidation is one order of magnitude slower in the post filter after partial aeration with high pH. Interestingly, the two lowest NH_4^+ oxidation rate constants were observed when there was no Mn^{2+} oxidation occurring.

4. Discussion

4.1. Controlling the NH_4^+ and Mn^{2+} oxidation sequence

The working hypothesis of this study was that by applying specific process conditions (O_2, pH) it is possible to control the sequence of Mn^{2+} and NH_4^+ oxidation in sand filters. All pilot filters were operated with mature filter sand, containing Mn-oxides as well as biofilms that were

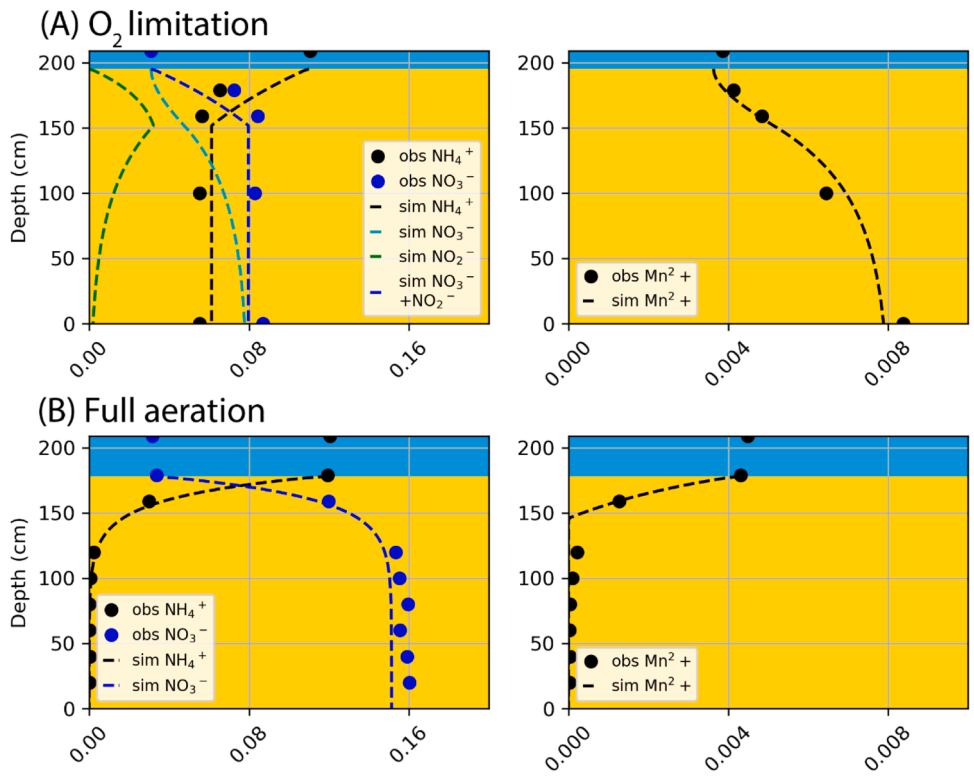

Fig. 7. Two model scenarios of pre-filter F4, where (A) shows the scenario where two-step nitrification is simulated during O_2 limitation in the pre-filter and (B) shows the scenario in the same pre-filter but during a temporarily operational period of full aeration.

Table 3
Estimated rate constants and adsorbed Mn^{2+} including their 95 % confidence intervals for the kinetic processes simulated by the reactive transport model for the different filters.

	Influent pH (-)	Influent O_2 concentrations (mmol/L)	NH_4^+ oxidation (s^{-1})	NH_4^+ oxidation – 95 % confidence limits (s^{-1})	Adsorbed Mn^{2+} (mmol/L)	Adsorbed Mn^{2+}– 95 % confidence limits (mmol/L)
F1– Simultaneous $Mn^{2+}$and NH_4^+ oxidation	8.00	0.33	3.5×10^{-2}	3.3×10^{-2}–3.7×10^{-2}	1.2×10^{-3}	1.1×10^{-3}–1.35×10^{-3}
F2 – Sequential Mn^{2+} and NH_4^+oxidation	7.74	0.08	0	-	1.4×10^{-2}	1.0×10^{-2}–1.7×10^{-2}
F3 – Sequential Mn^{2+} and NH_4^+oxidation	8.08	0.32	6.8×10^{-3}	1.4×10^{-3}–1.2×10^{-2}	-	-
F4 – Sequential $NH_4^+$and Mn^{2+} oxidation	6.88	0.12	5.5×10^{-3}	4.2×10^{-3}–7.0×10^{-3}	0	-
F5 – Sequential $NH_4^+$and Mn^{2+} oxidation	7.88	0.35	2.9×10^{-2}	2.7×10^{-2}–3.1×10^{-2}	2.5×10^{-3}	2.3×10^{-3}–2.6×10^{-3}

capable of oxidizing NH_4^+ and NO_2^-. As such, the conditions were present in all filters to oxidize both contaminants in an effective manner. Under saturated O_2 concentrations (10 mg/L) and high pH (±8), indeed both NH_4^+ and Mn^{2+} were oxidized from day 1, with NH_4^+ oxidation rate constant of 3.5×10^{-2} s^{-1} and adsorbed Mn^{2+}(a proxy for the heterogeneous Mn^{2+} oxidation rate) of 1.2×10^{-3} mmol/L. Under O_2 limiting conditions, however, it was possible to separate the two oxidation processes.

Theoretically, chemical heterogeneous Mn^{2+} is slowed down by a factor 825 at a low pH (pH~6.8) compared to a high pH after full aeration (pH~8), according to the rate equation proposed by Davies and Morgan (1989). In this way, Mn^{2+}oxidation was effectively suppressed at low pH in pre-filter F4, while NH_4^+ oxidizing bacteria utilised the limited O_2 available. Nonetheless, these conditions also resulted in a lower NH_4^+ oxidation rate constant (5.5×10^{-3} s^{-1} compared to 3.5×10^{-2} s^{-1} in the fully aerated filter F1) (Table 3).

We demonstrated control over this oxidation sequence by reversing the order of $NH_4^+$and Mn^{2+}oxidation, allowing $Mn^{2+}$to oxidize before NH_4^+. To achieve this uncommon sequence, the pre-filter F2 was operated with low O_2 concentrations (~0.017 mmol/L, 0.54 mg/L) and a high pH (~8). The O_2 concentration was sufficient to oxidize all Mn^{2+}, whereas ~18 times more O_2 (~0.3 mmol/L) would have been required for complete nitrification. Furthermore, the high pH favoured and accelerated heterogeneous Mn^{2+} oxidation (Davies and Morgan, 1989). The pH in this system was as high as the one in the fully aerated filter, where NH_4^+ is completely oxidized, suggesting that the adjusted O_2 concentration was the key factor to suppress NH_4 oxidation and allow Mn^{2+} oxidation.

It must be noted that accurate pH and O_2 control played a central role in the set-up. If the pH is too high, precipitation of calcite and potentially other minerals can accelerate sand filter clogging. Similarly, O_2 control is crucial: insufficient O_2 results in residual reductants in the next filter, while excessive O_2 potentially initiates oxidation of other reductants in the filter. Therefore, monitoring and process control are necessary during the start-up of a sequential Fe^{2+}, Mn^{2+}, and NH_4^+ oxidizing filter. Adjustments can be made in the filter based on the monitoring data. For example, aeration can be reduced or increased depending on the effluent concentrations of the separate filters.

4.2. Ammonium – manganese interactions

Mn^{2+} concentrations increased in pre-filter F4. Its mobilization poses a risk to RSF operation, as the elevated Mn^{2+} concentrations in the effluent water counteract the primary function of RSFs to remove Mn^{2+}. Model simulations indicate that this increase was potentially caused by NO_2^- dependent reduction of Mn-oxides. This interpretation is consistent with the observations of Vandenabeele et al. (1995), who reported chemical interactions between NO_2^- and Mn-oxides in batch experiments. In theory, abiotic or biotic oxidation of organic matter can also be coupled to MnO_2 reduction (Gounot, 1994; Remucal and Ginder-Vogel, 2014). In groundwaters, reduction generally follows a sequence, where reduction of MnO_2 only starts after the reduction of the more energetically favorable O_2 or NO_3^- (Appelo and Postma, 2004). This makes the reduction of MnO_2 coupled to organic matter oxidation less likely in F4, as O_2 or NO_3^- is always present. Furthermore, anaerobic groundwaters are often low in reactive organic carbon due to prior aerobic oxidation during infiltration (Hartog et al., 2004). Assimilable organic carbon (AOC) represents the fraction of dissolved organic carbon that can be readily taken up and metabolized by microorganisms. Anaerobic groundwater is generally characterized by low AOC concentrations (<10 μg/L in the Netherlands (van der Kooij et al., 1982), on average 60 μg/L and up to 114 μg/L in Flanders, Belgium (Polanska et al., 2005)). While organic matter oxidation coupled to MnO_2 reduction cannot be excluded, environmental conditions (presence of O_2, NO_3^-, and low AOC) indicate that NO_2^--dependent Mn oxide reduction is the most probable pathway.

In conventional RSFs, where sufficient O_2 is present, the NO_2^- resulting from NH_4^+ oxidation is quickly microbially converted to NO_3^-. In pre-filter F4, where the concentration of O_2 was insufficient to fully oxidize NH_4^+ to NO_3^-, the Mn-oxides present seem to react with the formed NO_2^-. Interestingly, Vandenabeele et al. (1995), performed a similar experiment with limiting O_2 at a higher pH (7.7), which is a more regularly observed influent pH in RSFs, and observed that Mn-oxide reduction did not occur. These observations seem to indicate that NO_2^--dependent Mn-oxide reduction is only a risk, when (i) the pH is relatively low, (ii) incomplete NH_4^+ oxidation is occurring resulting in NO_2^- due to O_2 depletion, and (iii) Mn-oxide coated sand is present as in the current study. These conditions are not rare in conventional RSFs and could explain the ever-lasting problem of Mn^{2+} breakthrough faced by drinking water utilities (Bruins et al., 2013; Haukelidsaeter et al., 2023). The easiest way to eliminate NO_2^- dependent Mn-oxide reduction and the subsequent mobilization of Mn^{2+} is to use virgin sand instead of Mn-oxide coated sand for future sequential oxidizing filters.

Parameter estimation highlighted potential interactions between NH_4^+ and Mn^{2+} affecting oxidation rates. First, we observed that Mn^{2+} oxidation proceeded about one order of magnitude faster in the absence of NH_4^+, despite the slightly lower pH and O_2 concentration. Faster oxidation of Mn^{2+} in the absence of NH_4^+ could be related to their competition for O_2 for oxidation, as NH_4^+ oxidation is a more favorable redox reaction compared to Mn^{2+} oxidation. Second, faster NH_4^+ oxidation was observed when simultaneously Mn^{2+} oxidation was occurring. Recent studies in constructed wetlands for treating wastewater showed that 92 % of the Mn^{2+}-oxidizing bacteria could potentially play a role in the nitrogen cycle and that NH_4^+ oxidation was closely related to Mn-oxides and Mn^{2+} concentrations (Cheng et al., 2022; Wang et al., 2021). These findings highlight the interconnection between NH_4^+ and Mn^{2+} oxidation, however, further research on these potential interactions is needed to validate the outcomes of the current study and to assess the specific mechanisms.

4.3. Outlook

To the best of our knowledge, this is the first study that demonstrates the sequential oxidation of Fe^{2+}, Mn^{2+}, and NH_4^+ in three separate filters and that the sequence of Mn^{2+} and NH_4^+ oxidation is interchangeable. We believe that sequential oxidation has the potential to improve system controllability and operating efficiency. However, this study only shows a proof of principle, and further research is needed before implementation in full-scale drinking water production. To guide the future development, we propose the following research lines:

1. Assess the long-term operational stability and optimal process conditions at demo-scale.
2. Compare functioning of sequential oxidation treatment with conventional aeration/filtration treatment.
3. Investigate practical issues for implementation, as optimal design, and costs of operation and maintenance.

From an operational perspective, the sequence in which NH_4^+ precedes Mn^{2+} oxidation is preferred, as it provides greater assurance of biological stability in treated groundwater (Prest et al., 2016). In this configuration, nitrification occurs prior to Mn^{2+} oxidation, allowing any minor NH_4^+ breakthroughs to be removed in the second filter. Thereby, decreasing the chance of residual NH_4^+ in the effluent water. Another benefit of this sequence is that it does not require chemicals. We believe that sequential oxidation is particularly relevant for new drinking water treatment plants, as the single or dual media filter configurations in existing plants are not compatible with a three-filter sequential oxidation system. Constructing a new plant allows for smaller sequential filters while maintaining flexibility for operational adjustments. Although three filters are needed for treatment by sequential oxidation instead of one for conventional treatment, the plant footprint potentially can stay similar, as the likely higher flows and reaction rates enable using smaller sized filters. However, further research on this is needed.

5. Conclusions

We demonstrated that the main anaerobic groundwater contaminants, namely Fe^{2+}, NH_4^+, and Mn^{2+}, can be oxidized sequentially in separate filters; and that the common order of NH_4^+ before Mn^{2+} oxidation can be reversed to allow Mn^{2+} to oxidize first. These atypical oxidation dynamics were driven by low O_2 concentrations (~0.017 mmol/L, ~0.54 mg/L) and a high pH (~8), which strongly favoured Mn^{2+} oxidation, leading to rapid O_2 depletion which suppressed NH_4^+ oxidation. The opposite occurred in the filter with low O_2 concentrations (0.08 mmol/L, ~3 mg/L) and low pH (~6.8) where Mn^{2+} oxidation was inhibited, enabling NH_4^+-oxidizing bacteria to consume all O_2. This shift from conventional anaerobic groundwater treatment with simultaneous oxidation to sequential oxidation in separate filters can result in (i) a more robust and controllable system, (ii) the potential to optimize the rates of each oxidation process separately, and (iii), ultimately, higher flows and less backwashing. However, further research is needed before implementation in full-scale drinking water production on long-term stability, optimal process conditions and design, and costs of operation and maintenance.

CRediT authorship contribution statement

Emiel Kruisdijk: Writing – review & editing, Writing – original draft, Visualization, Software, Methodology, Formal analysis, Data

curation. **Francesc Corbera-Rubio:** Writing – review & editing, Writing – original draft, Methodology, Investigation, Formal analysis, Conceptualization. **Simon Müller:** Writing – review & editing, Methodology, Investigation, Conceptualization. **Frank Schoonenberg:** Resources, Methodology, Conceptualization. **Michele Laureni:** Writing – review & editing, Writing – original draft, Methodology, Conceptualization. **Melanie Nijboer:** Methodology, Investigation, Data curation. **Doris van Halem:** Writing – review & editing, Writing – original draft, Project administration, Methodology, Investigation, Funding acquisition, Formal analysis, Conceptualization.

Declaration of competing interest

The authors declare that they have no known competing financial interests or personal relationships that could have appeared to influence the work reported in this paper.

Supplementary materials

Supplementary material associated with this article can be found, in the online version, at doi:10.1016/j.watres.2026.125436.

Data availability

Data will be made available on request.

References

Appelo, C.A.J., Postma, D., 2004. Geochemistry, Groundwater and Pollution. CRC press.

Bruins, J.H., Petrusevski, B., Slokar, Y.M., Huysman, K., Joris, K., Kruithof, J.C., Kennedy, M.D., 2015. Biological and physico-chemical formation of Birnessite during the ripening of manganese removal filters. Water Res. 69, 154–161. https://doi.org/10.1016/j.watres.2014.11.019.

Bruins, J.H., Vries, D., Petrusevski, B., Slokar, Y.M., Kennedy, M.D., 2013. Assessment of manganese removal from over 100 groundwater treatment plants. J Water Supply: Res. Technol.-Aqua 63 (4), 268–280. https://doi.org/10.2166/aqua.2013.086.

Cheng, C., He, Q., Zhang, J., Chai, H., Yang, Y., Pavlostathis, S.G., Wu, H., 2022. New insight into ammonium oxidation processes and mechanisms mediated by manganese oxide in constructed wetlands. Water Res. 215, 118251. https://doi.org/10.1016/j.watres.2022.118251.

Corbera-Rubio, F., Goedhart, R., Laureni, M., van Loosdrecht, M.C.M., van Halem, D., 2024a. A biotechnological perspective on sand filtration for drinking water production. Curr. Opin. Biotechnol. 90, 103221. https://doi.org/10.1016/j.copbio.2024.103221.

Corbera-Rubio, F., Kruisdijk, E., Malheiro, S., Leblond, M., Verschoor, L., Loosdrecht, M.C.M.v., Laureni, M., Halem, D.v., 2024b. A difficult coexistence: resolving the iron-induced nitrification delay in groundwater filters. bioRxiv. https://doi.org/10.1101/2024.02.19.581000, 2024.2002.2019.581000.

Davies, S.H.R., Morgan, J.J., 1989. Manganese(II) oxidation kinetics on metal oxide surfaces. J Colloid Interface Sci 129 (1), 63–77. https://doi.org/10.1016/0021-9797(89)90416-5.

Diem, D., Stumm, W., 1984. Is dissolved Mn2+ being oxidized by O2 in absence of Mn-bacteria or surface catalysts? Geochim. Cosmochim. Acta 48 (7), 1571–1573. https://doi.org/10.1016/0016-7037(84)90413-7.

Doherty, J., 1994. PEST: Model Independent parameter Estimation (W. Computing, Ed.).

Emerson, D., De Vet, W., 2015. The role of FeOB in engineered water ecosystems: a review. J. AWWA 107 (1), E47–E57. https://doi.org/10.5942/jawwa.2015.107.0004.

Fetter, C.W., Boving, T.B., Kreamer, D.K., 1999. *Contaminant Hydrogeology* (Vol. 500). Prentice hall Upper Saddle River, NJ.

Gounot, A.-M., 1994. Microbial oxidation and reduction of manganese: consequences in groundwater and applications. FEMS Microbiol. Rev. 14 (4), 339–349. https://doi.org/10.1111/j.1574-6976.1994.tb00108.x.

Hartog, N., Van Bergen, P.F., De Leeuw, J.W., Griffioen, J., 2004. Reactivity of organic matter in aquifer sediments: geological and geochemical controls. Geochim. Cosmochim. Acta 68 (6), 1281–1292. https://doi.org/10.1016/j.gca.2003.09.004.

Haukelidsaeter, S., Boersma, A.S., Kirwan, L., Corbetta, A., Gorres, I.D., Lenstra, W.K., Schoonenberg, F.K., Borger, K., Vos, L., van der Wielen, P.W.J.J., van Kessel, M.A.H.J., Lücker, S., Slomp, C.P., 2023. Influence of filter age on Fe, Mn and NH4+ removal in dual media rapid sand filters used for drinking water production. Water Res. 242, 120184. https://doi.org/10.1016/j.watres.2023.120184.

Haukelidsaeter, S., Boersma, A.S., Piso, L., Lenstra, W.K., van Helmond, N.A.G.M., Schoonenberg, F., van der Pol, E., Hurtarte, L.C.C., van der Wielen, P.W.J.J., Behrends, T., van Kessel, M.A.H.J., Lücker, S., Slomp, C.P., 2024. Efficient chemical and microbial removal of iron and manganese in a rapid sand filter and impact of regular backwash. Appl. Geochem. 162, 105904. https://doi.org/10.1016/j.apgeochem.2024.105904.

Kaegi, R., Voegelin, A., Folini, D., Hug, S.J., 2010. Effect of phosphate, silicate, and Ca on the morphology, structure and elemental composition of Fe(III)-precipitates formed in aerated Fe(II) and As(III) containing water. Geochim. Cosmochim. Acta 74 (20), 5798–5816. https://doi.org/10.1016/j.gca.2010.07.017.

Kappler, A., Bryce, C., Mansor, M., Lueder, U., Byrne, J.M., Swanner, E.D., 2021. An evolving view on biogeochemical cycling of iron. Nat. Rev. Microbiol. 19 (6), 360–374. https://doi.org/10.1038/s41579-020-00502-7.

van der Kooij, D., Visser, A., Hijnen, W.A.M., 1982. Determining the concentration of easily assimilable organic carbon in drinking water. J. AWWA 74 (10), 540–545. https://doi.org/10.1002/j.1551-8833.1982.tb05000.x.

Kruisdijk, E., van Breukelen, B.M., van Halem, D., 2024. Simulation of rapid sand filters to understand and design sequential iron and manganese removal using reactive transport modelling. Water Res. 267, 122517. https://doi.org/10.1016/j.watres.2024.122517.

Müller, S., Corbera-Rubio, F., Schoonenberg-Kegel, F., Laureni, M., Loosdrecht, M.C.M. v., Halem, D.v., 2024. Shifting to biology promotes highly efficient iron removal in groundwater filters. bioRxiv. https://doi.org/10.1101/2024.02.14.580244, 2024.2002.2014.580244.

Parkhurst, D.L., Appelo, C.A.J., 2013. *Description of input and examples for PHREEQC version 3: a computer program for speciation, batch-reaction, one-dimensional transport, and inverse geochemical calculations* [Report](6-A43). (Techniques and Methods, Issue. U. S. G. Survey. http://pubs.er.usgs.gov/publication/tm6A43.

Polanska, M., Huysman, K., van Keer, C., 2005. Investigation of assimilable organic carbon (AOC) in flemish drinking water. Water Res. 39 (11), 2259–2266. https://doi.org/10.1016/j.watres.2005.04.015.

Prest, E.I., Hammes, F., van Loosdrecht, M.C.M., Vrouwenvelder, J.S., 2016. Biological stability of drinking water: controlling factors, methods, and challenges. Front. Microbiol. 7. https://doi.org/10.3389/fmicb.2016.00045.

Remucal, C.K., Ginder-Vogel, M., 2014. A critical review of the reactivity of manganese oxides with organic contaminants [10.1039/C3EM00703K]. Environ. Sci.: Process. Impact. 16 (6), 1247–1266. https://doi.org/10.1039/C3EM00703K.

Stumm, W., Lee, G.F., 1961. Oxygenation of ferrous iron. Ind. Eng. Chem. 53 (2), 143–146. https://doi.org/10.1021/ie50614a030.

Tatari, K., Smets, B.F., Albrechtsen, H.J., 2013. A novel bench-scale column assay to investigate site-specific nitrification biokinetics in biological rapid sand filters. Water Res. 47 (16), 6380–6387. https://doi.org/10.1016/j.watres.2013.08.005.

Tekerlekopoulou, A.G., Pavlou, S., Vayenas, D.V., 2013. Removal of ammonium, iron and manganese from potable water in biofiltration units: a review. J. Chem. Technol. Biotechnol. 88 (5), 751–773. https://doi.org/10.1002/jctb.4031.

UNESCO. (2022). The United Nations World Water Development Report 2022: Groundwater: Making the invisible visible.

Vandenabeele, J., Vande Woestyne, M., Houwen, F., Germonpré, R., Vandesande, D., Verstraete, W., 1995. Role of autotrophic nitrifiers in biological manganese removal from groundwater containing manganese and ammonium. Microb. Ecol. 29 (1), 83–98. https://doi.org/10.1007/BF00217425.

Voegelin, A., Kaegi, R., Frommer, J., Vantelon, D., Hug, S.J., 2010. Effect of phosphate, silicate, and Ca on Fe(III)-precipitates formed in aerated Fe(II)- and As(III)-containing water studied by X-ray absorption spectroscopy. Geochim. Cosmochim. Acta 74 (1), 164–186. https://doi.org/10.1016/j.gca.2009.09.020.

Wang, D., Lin, H., Ma, Q., Bai, Y., Qu, J., 2021. Manganese oxides in phragmites rhizosphere accelerates ammonia oxidation in constructed wetlands. Water Res. 205, 117688. https://doi.org/10.1016/j.watres.2021.117688.